PACS numbers: 42.70.Mp
DOI: 10.1070/QE2007v037n05ABEH013307

Possibility of increasing the optical breakdown threshold in KDP crystals

V.I. Bredikhin, V.P. Ershov, V.N. Burenina, A.N. Mal'shakov, A.K. Potemkin

***Abstract*. The effect of various technological factors like the direction of crystal growth [(100) or (101)], acidity of the mother solution, growth rate, degree of filtration of the mother solution, purity of the starting raw material, specially introduced impurity (Pb), as well as after-growth thermal annealing, on the optical breakdown threshold of KDP crystals grown by the technique of rapid growth of profiled crystals is studied. It is shown that by using initial high-purity salts and fine filtration of solutions followed by after-growth annealing, it is possible to increase the optical breakdown threshold of profiled rapidly grown KDP crystals to values corresponding to the requirements of modern laser designs.**

Keywords: *high-power laser systems, nonlinear optical crystals, KDP crystals, optical breakdown threshold.*

1. Introduction

A KDP crystal and its deuterated analogue – a DKDP crystal remain the main nonlinear optical materials used in high-power laser systems. They are widely used for frequency conversion and to control the pulse duration in laser devices for inertial confinement fusion (ICF) [1, 2]. Since its first application in nonlinear optics [3 – 5], the laser damage threshold of KDP has been studied extensively by various research groups [6 – 22] *. It was shown in a number of papers that the laser breakdown threshold depends on the crystal quality and the laser radiation parameters. The latter circumstance imposes stringent requirements on the quality of laser radiation in quantitative measurements of laser damage threshold and necessitates the use of single-mode single-frequency lasers whose power is sufficient for breakdown in a beam of diameter no less than 0.1 mm. In this case, measures should be taken to prevent self-focusing of the laser beam in the sample under study.

The quality of the crystal and improvement of the technique of its growth have a decisive influence on the laser damage threshold. Thus, it was found in [6] that the optical stability of a KDP crystal irradiated by the first and second harmonics of an Nd laser is determined by the defect structure of the crystal, in particular, by the size and type of microscopic inclusions. It was shown in [17 – 19, 21] that the optical stability of crystals can be improved considerably by processing crystals after their growth, either by exposing them to laser pulses of underbreakdown intensity or subjecting to thermal annealing.

Investigations of the laser damage threshold of KDP and DKDP crystals and the enhancement of laser breakdown threshold over a wide frequency range still remain of current interest. This is explained by an increase in the power and energy of laser radiation due to the advancements in the laser technology and in the crystal growth technique. At present, the aperture of the optical elements used in ICF systems is 40×40 cm, while the radiation energy density transmitted through these elements achieves 10 J cm^{-2} (for a pulse duration of ~ 1 ns) in the wavelength range 0.3 – 1.3 μm [1, 2, 18, 19, 21, 23, 24].

Although KDP crystals can be easily grown from solutions (which is the main advantage of these crystals over other nonlinear optical crystals), their cost proves to be very high. Therefore, it is extremely important to develop new efficient technologies of crystal growth and to improve the reliability of technologies and methods providing the required optical stability of crystals. At present, high-speed growth techniques, in which the crystal growth time is reduced by an order of magnitude and the size of the crystals can be drastically increased without any significant deterioration of their quality, find increasing applications [1, 2, 22, 25, 26]. Examples of using KDP and DKDP crystals obtained by fast growth of profiled crystals (matching the geometry of the optical element for which they are intended) for controlling laser radiation with energy at the level of kilojoules are presented in [23, 24, 27]. In particular, an example of the use of profiled 'rapidly grown' DKDP crystals for parametric generation of terawatt femtosecond pulses is given in [27].

The laser damage threshold of crystals obtained by the technique of high-speed growth of full-faceted crystals [1] was studied in several works (see, for example, [1, 18, 19, 21]), where it was shown that for optimal parameters of high-speed growth, the laser damage threshold of rapidly grown crystals does not differ from that of the best crystals grown by the traditional technique.

In this paper, we present the results of investigation of the laser damage threshold of KDP crystals obtained by the technique of high-speed growth of profiled crystals [2, 22, 25, 26]. The effect of some technological regimes

* This, however is not a complete list of all the papers on this subject because we did not intend to present a complete review of studies on laser stability of crystals.

V.I. Bredikhin, V.P. Ershov, V.N. Burenina, A.N. Mal'shakov, A.K. Potemkin Institute of Applied Physics, Russian Academy of Sciences, ul. Ul'yanova 46, 603950 Nizhnii Novgorod, Russia; e-mail: bredikh@appl.sci-nnov.ru

Received 16 June 2006; revision received 13 December 2006
Kvantovaya Elektronika **37** (5) 489 – 494 (2007)
Translated by Ram Wadhwa

and methods on the optical breakdown threshold at the Nd laser wavelength 1.054 μm and its third harmonic is studied. Special attention was paid to the parameters and technological methods whose importance had been established either in earlier publications [1, 2, 6–21], or by *a priori* considerations. The effect of the following parameters was studied: direction of crystal growth [growth of one face (101) of a bipyramid or one face (100) of a prism], acidity of the mother solution, the growth rate R, the degree of filtration of the mother solution, the purity of the starting materials and specially introduced impurity (Pb), as well as the post-growth thermal annealing of the crystals. The role of each of the factors was studied when the remaining factors were not changed.

2. Experimental

2.1 Crystal growth

KDP crystals were grown by the technique of high-speed growth of profiled crystals in a device of volume 10 L, which was described earlier in [2]. The crystals had a cross section of 43×43 mm and were up to 50 mm in length. The growth rate was varied in the interval 0.08–2.3 mm h^{-1}, and the crystals were grown with the face (100) or (101). The hydrodynamic growth regimes in all the experiments were identical. Solutions were prepared by the same method, and the saturation temperature determined by laser interferometry was $\sim 40\,^{\circ}C$. The acidity of solutions was controlled by adding H_3PO_4 acid (analytical grade). The Pb impurity was introduced in the working solution in the form of the acidic $Pb_3(PO_4)_2$ solution. Filtration was performed while pouring the supersaturated solution into the growth section through various filters: a bulk fluoroplastic filter with the porosity $d = 10$ μm, a membrane Sartorius filter (PTFE) with the porosity $d = 0.2$ μm, and a Vladipor filter (MFFK) with the porosity $d = 0.3 - 0.7$ μm, and through track membranes with $d = 0.3 - 0.67$ μm. Two different batches of the initial KH_2PO_4 salt produced by the Research Institute of Single Crystals (Ukraine) (high purity salt – HP-16) and ProChem (USA) [LLNL grade (ProChem salt)] were used. The latter batch was specially developed for the high-speed growing of high-quality crystals. The growth rate could be varied during one experiment without interruption and in different experiments.

2.2 After-growth annealing of crystals

Crystals were annealed in a computer-controlled oven with stepwise raising and lowering of temperature and holding at a maximum temperature of 150 °C. The total annealing time was five days.

2.3 Measurement of the laser damage threshold

We measured the laser damage threshold at the first (ω) and the third (3ω) harmonics of a 1.054-μm Nd phosphate glass laser. Figure 1 shows the scheme of the experimental setup. The setup consisted of master oscillator (MO) *I*, circuit *II* for the formation of spatial and temporal characteristics of the radiation, amplifier *III*, radiation frequency converter *IV*, and dust-proof chamber *V* containing the sample under study.

The laser was designed to provide radiation with controllable parameters, because the spatial and temporal dependence of the radiation intensity have to be controlled

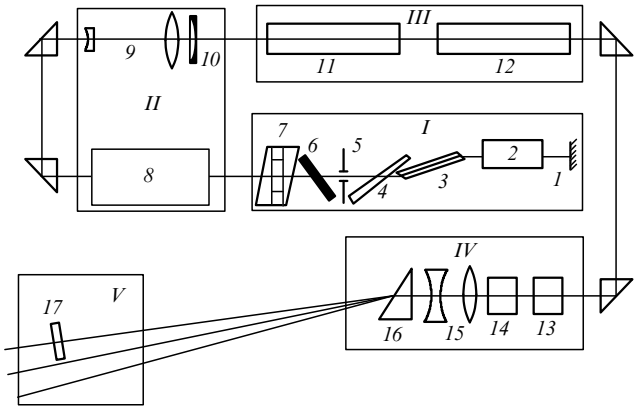

Figure 1. Optical scheme of the experimental setup; (*I*) master oscillator; (*1*) highly reflecting mirror; (*2*) interference-polarisation filter (Wood filter); (*3*) GLS 22P glass active element; (*4*) calcite wedge; (*5*) 1.8-mm diaphragm; (*6*) passive saturable dye Q-switch; (*7*) stack; (*II*) scheme for the formation of temporal and spatial characteristics of radiation; (*8*) single pulse selector; (*9*) $5^{\times}$ telescope; (*10*) apodising diaphragm; (*III*) amplifier with phosphate glass active elements (*11*) and (*12*); (*IV*) system for probe radiation formation; (*13*, *14*) second and third harmonic DKDP generators with the type I (ooe) phase matching; (*15*) telescopic objective; (*16*) dispersion prism; (*V*) dust-proof chamber with sample (*17*).

in the plane of a sample. This can be achieved by using Gaussian beams with a smooth time dependence of intensity. Because it is difficult to measure the time dependence of the parameters of single pulses with a resolution better than 0.1–0.2 ns, we also monitored the spectral characteristics of radiation.

Master oscillator *I* (Fig. 1) was passively self-mode-locked and emitted single pulses every five minutes. Active laser element (*3*) of diameter 10 mm and length 160 mm was fabricated from a GLS22P neodymium phosphate glass. To prevent reflection from the end faces of the active element, they were cut at the Brewster angle. The active element was pumped by flash lamps mounted in an elliptical mirror reflector. The laser was Q-switched by using a saturable 7294U dye in isopropyl alcohol. The solution was poured into cell (*6*) of thickness 1 mm, inclined to the axis at the Brewster angle.

The MO cavity of length 1.8 mm consisted of plane mirror (*1*) and stack (*7*) formed by two planes separated by a 2-cm air gap. The stack provided a constant air gap in a broad temperature range. Thermally stabilised Wood interference–polarisation filter (*2*) [28], which was used as a Fabry–Perot resonator, provided, in conjunction with the cavity, single-frequency lasing. In all the cases, the emission spectrum consisted of a single line of width ~ 0.02 cm^{-1}, which remained fixed from pulse to pulse. The linewidth and the absence of side satellites demonstrate the smoothness of the pulse envelope in time. Frequency stabilisation was especially important to stabilise the third harmonic generation. The single (zeroth) transverse mode was selected by diaphragm (*5*) of diameter 1.8 mm. Calcite optical wedge (*4*) provided a high degree of polarisation of the MO radiation.

The MO emitted a train of 10–15 pulses. System *II* for the formation of temporal and spatial characteristics of radiation included selector (*8*) of single pulses, telescopic beam expander (*9*) and apodising diaphragm (*10*). The pulse selector consisted of a spark-gap-controlled Pockels

cell, which was triggered by laser radiation. The response time of this gate was ~ 1 ns, which is sufficient for selecting a single pulse from the pulse train.

Because it is desirable to have a Gaussian transverse intensity distribution in the sample plane, we used soft diaphragm (*10*) (Fig. 1) with a Gaussian transmission profile. To match the MO beam diameter with those of amplifiers (*11*) and (*12*), beam-expanding Galilean telescope (*9*) was used. Flash-pumped amplifiers with phosphate glass active elements of diameter 20 mm and length 250 mm provided the output energy in a single pulse up to 1 J, thus making it possible to measure the laser damage threshold for a characteristic diameter of the illuminated region up to 2 mm in samples with the laser damage threshold up to 30 J cm^{-2}. The transverse output intensity distribution was close to the Gaussian distribution $I(r) = I_0 \times \exp[-(r/r_0)^2]$ with $r_0 = 0.54$ m. A similar setup was described in detail in [29].

The second and third harmonic generators consisted of two 4-cm long DKDP crystals cut at the type I phase-matching angle. The crystals were oriented as in the scheme in [30].

Radiation was focused on a sample by using two-component telescopic objective (*15*) with a variable focal length (~ 4 m), which produced an illuminated spot of required size on the plane of the sample. Silica dispersion prism (*16*) separated beams with frequencies ω, 2ω and 3ω in space. The focal length of objective (*15*) used in measurements of laser damage threshold of the crystals was 350 cm. The length of the beam waist for the first, second and third harmonic was 96, 49 and 31 cm, respectively. The intensity distribution was nearly Gaussian, with the beam diameter at the e^{-2} level being 0.8, 0.4 and 0.26 mm, respectively. In view of the relatively large beam diameter at the focus, we can expect representative results for large-size crystals and high-power laser beams of large diameter.

A reference sample was prepared for measuring the laser damage threshold of transparent dielectrics. The sample aperture was 40×40 mm and its thickness L was 10 mm. The reference sample thickness was chosen in such a way as to minimise the effect of self-focusing on the geometry of the radiation during its propagation through the sample. The smallness criterion can be estimated from the value of the B integral over the length of the sample. For a Gaussian beam of power P propagated through a nonlinear layer of thickness of L, we have

$$B = \frac{P}{P_{cr}} \frac{2}{n} \frac{L}{z_d},$$

where n is the refractive index of the material of the sample, z_d is the length of diffraction spread of the beam in the sample plane, and P_{cr} is the critical power of self-focusing in the sample material. For most of the transparent dielectrics, the critical power P_{cr} lies in the range 1–4 MW [31]. For our geometry of radiation in the plane of a sample of thickness $L = 1$ cm at a maximum intensity $I = 20$ GW cm^{-2}, the values of the B integral are 0.1–0.35, which is much smaller than the value $B = 1 - 3$ at which the nonlinearity of the sample material may affect the geometry of beam propagation [31].

Similar estimates for the second and third harmonics show that the effect of self-focusing on the measuring conditions is negligible.

Measurements were performed by irradiating samples by a single pulse, irrespective of the presence of damage. The breakdown was detected by the appearance of new defects in the irradiated volume observed in scattered light under a $40^{\times}$ microscope. Irrespective of whether the sample was damaged or not, it was displaced by 2 mm after each flash, and the irradiated region was observed in strongly scattered light through an MBS-1 binocular microscope. Any difference in the patterns observed through the microscope before and after the flash was treated as damage. About 30–50 flashes were required for each sample for determining its mean breakdown threshold W_{th}.

The laser pulse duration used in our studies was varied between 0.7 and 1.5 ns. All the results of laser damage threshold measurements were scaled to the empirical root dependence of the threshold damage intensity on time $I_{th}(r) = I_{th}(\tau = 1\text{ ns})\tau^{-1/2}$, where $I_{th}(\tau = 1\text{ ns})$ is the breakdown threshold intensity for the pulse duration $\tau = 1$ ns [32]. In this interval of pulse durations, the root dependence weakly differs from the theoretical dependence [33, 34] for the breakdown threshold at the absorbing microinclusions. If the radiation intensity in each flash is not scaled to a root dependence, the breakdown threshold cannot be determined unambiguously. Hereafter in this text, the breakdown threshold is defined as the breakdown threshold energy density $W_{th} = W_{th}(\tau = 1\text{ ns})$.

The systematic error in determining the breakdown threshold depends mainly on the error ($\pm 20\,\%$) of the calorimeter used for measurements. The random error estimated from the spread of the experimental points was $\pm 10\,\%$. To compare the results and to ensure the possibility of repeating the measurements, the optical breakdown threshold of KU-1 silica was measured in each series.

3. Experimental results

The dependence of the laser breakdown threshold on various technological factors and regimes are presented in Figs 2–9 in the form of diagrams, which also show the optical breakdown threshold of KU-1 silica.

For KDP crystals grown along the face (100), measurements were performed only at the first harmonic because these crystals have considerable absorption at the third harmonic [25] and it is not expedient to use them in this spectral region.

The main results of our measurements can be summarised as follows:

(i) The laser breakdown threshold is independent of the solution acidity (Fig. 2). This is reasonable because acid does not enter the crystal.

(ii) The laser breakdown threshold is independent of the rate R of crystal growth over a wide range $R = 0.08 - 2.3$ mm h^{-1} (Fig. 3). This means that an increase in the growth rate under optimal hydrodynamic conditions does not produce new defects. Note that the value $R = 0.8$ mm h^{-1} is close to the growth rate in the conventional technology, thus indicating that the structures of crystals grown by conventional and high-speed growth techniques are identical.

(iii) The laser breakdown thresholds for crystals with orientations (100) and (101) at 1.054 μm do not differ significantly (Fig. 4), i.e. the impurities determining UV absorption in crystals with orientation (100) do not affect the breakdown threshold at this wavelength.

(iv) Crystals grown from the ProChem salt have a higher

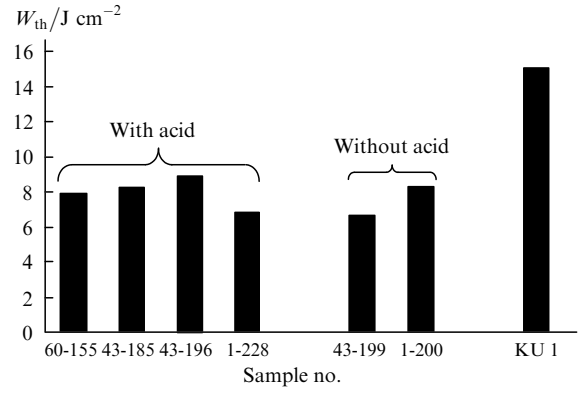

Figure 2. The first-harmonic laser breakdown threshold W_{th} for crystals grown in stoichiometric solutions and with the addition of acid.

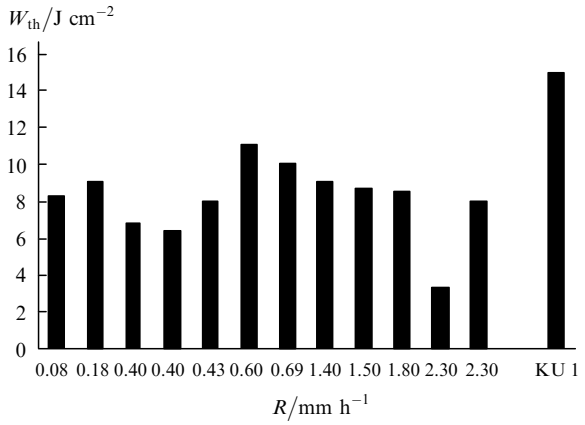

Figure 3. Effect of growth rate R on the first-harmonic laser breakdown threshold W_{th}.

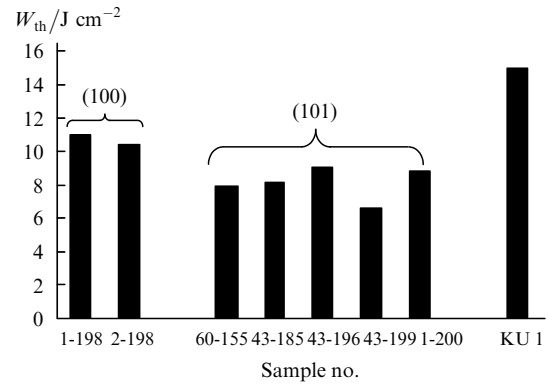

Figure 4. The first-harmonic laser breakdown threshold W_{th} for crystals with orientation (100) and (101).

optical breakdown threshold consistently as compared to crystals grown from the HP-16 salt (Fig. 5). This is due to a higher purity of the ProChem salt. For example, the ratings on the certificate of production show that the concentration of Fe in the ProChem salt is one-third of the concentration in the HP-16 salt. The so-called dead zone Δt_d [35] in the ProChem salt is also much smaller ($\Delta t_d \approx 0.3\,^\circ$C and $\sim 1\,^\circ$C in the ProChem and HP-16 salts, respectively).

(v) A finer filtration results in the increase in the breakdown threshold on the average (Fig. 6). However,

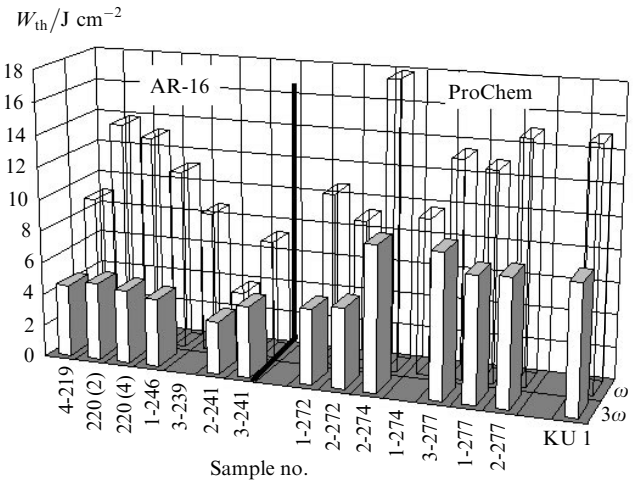

Figure 5. Effect of the initial salts [HP-16 and LLNL grade (ProChem)] on the first (ω) and third (3ω) harmonic laser breakdown threshold W_{th} (the bold line separates experiments with HP-16 and LLNL grade reagents).

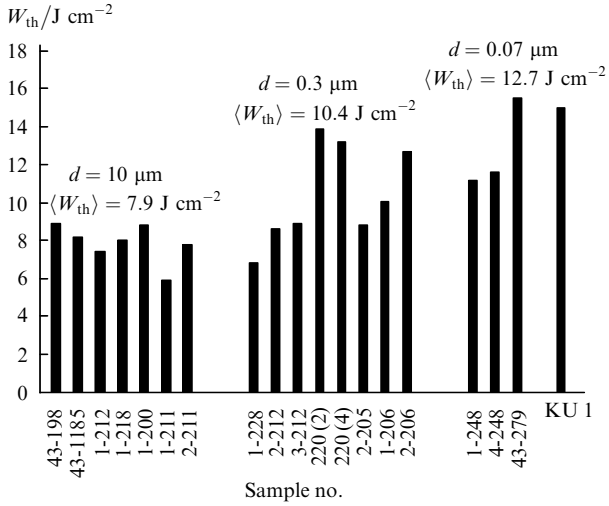

Figure 6. Dependence of the first-harmonic laser breakdown threshold W_{th} on the degree of filtration of the solution (fluoroplastic filter with a porosity $d = 10$ μm, and Vladipor filter with a porosity $d = 0.3$ and 0.07 μm). Angle brackets enclosing W_{th} indicate averaging over a batch of experiments with the given filter.

no drastic and stable increase in the threshold was observed. This is probably due to the presence of common contamination, which cannot be eliminated by a preliminary filtration of the solution.

(vi) The introduction of lead impurity with the optimal mass concentration $\sim 10^{-3}$ % can increase the breakdown threshold (see Fig. 7).

(vii) Thermal annealing of crystals leads to a considerable increase in the breakdown threshold (by a factor of 2.5–3; Figs 8 and 9). Crystals with lead impurity are an exception because their breakdown threshold does not increase after annealing.

4. Conclusions

Thus, by using initial high-purity salts and fine filtration of solutions (including filtration during the growth) together

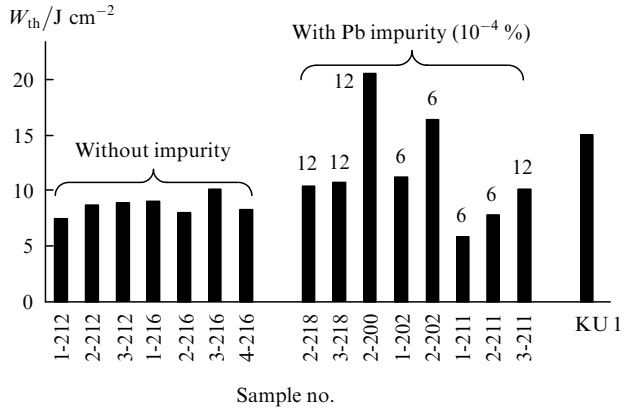

Figure 7. First-harmonic optical breakdown threshold W_{th} for crystals grown without impurities and with Pb impurity (the mass concentration of the Pb impurity in the solution in 10^{-4} % is indicated over the columns).

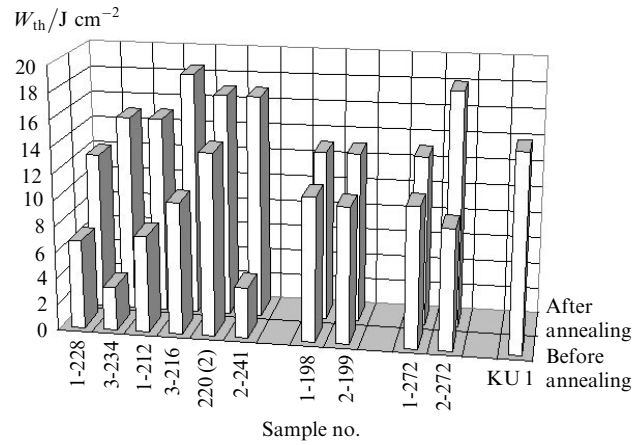

Figure 8. Effect of annealing on the first-harmonic laser breakdown threshold W_{th}.

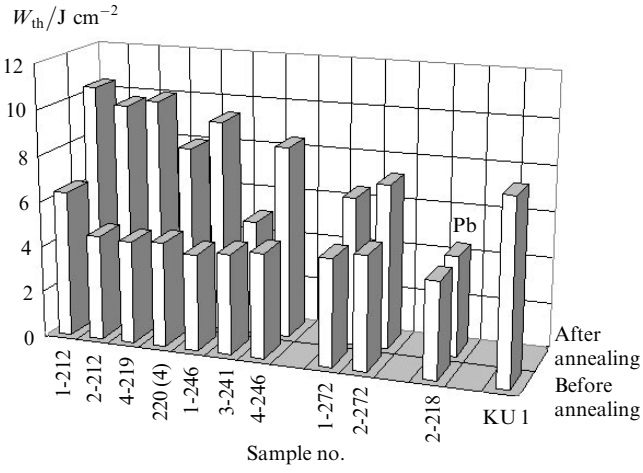

Figure 9. Effect of annealing on the third-harmonic laser breakdown threshold W_{th} (the 2-218 crystal was grown with the Pb impurity).

with the after-growth annealing of the crystals, the laser damage threshold of profiled KDP crystals grown at a high speed can be increased to meet the requirements of modern laser projects.

References

1. Zaitseva N., Atherton J., Rozsa R., Smolsky I., Carman L., Runkel M., Ryon R., James L. *J. Cryst. Growth*, **197**, 911 (1999).
2. Bespalov V.I., Bredikhin V.I., Ershov V.P., Zilberberg V.V., Katsman V.I. *Proc. SPIE Int. Soc. Opt. Eng.*, **4424**, 124 (2001).
3. Giordmaine J.A. *Phys. Rev. Lett.*, **8**, 19 (1962).
4. Maker P.D., Terhune R.W., Nisenoff M., Savage C.M. *Phys. Rev. Lett.*, **8**, 21 (1962).
5. Terhune R.W., Maker P.D., Savage C.M. *Appl. Phys. Lett.*, **2**, 54 (1963).
6. Batyreva I.A., Bespalov V.I., Kiselev A.M., Miller A.M. *Kvantovaya Elektron.*, **5**, 1838 (1978) [*Sov. J. Quantum Electron.*, **8**, 1044 (1978)].
7. Anan'ev O.B., Bykovskii Yu.A., Petrovskii A.N., Rez I.S. *Zh. Tekh. Fiz.*, **42**, 837 (1972).
8. Zverev G.M., Levchuk E.A., Maldutis E.K. *Zh. Eksp. Teor. Fiz.*, **57**, 730 (1969).
9. Endert H., Hattenbach A., Melle W. *Kvantovaya Elektron.*, **4**, 2653 (1977) [*Sov. J. Quantum Electron.*, **7**, 1516 (1977)].
10. Cristmas T.M., Ley N.M. *Electron. Lett.*, **7**, 544 (1971).
11. Melle W., Galler R. *Phys. Stat. Sol. (a)*, **58**, 167 (1980).
12. Wax S.I., Chodorow M., Puthov H.E. *Appl. Phys. Lett.*, **16**, 157 (1970).
13. Newkirc H., Swain J., Stokowski S., Milam D., Klapper H. *J. Cryst. Growth*, **65**, 651 (1983).
14. Genkin V.N., Miller A.M., Soustov L.V. *Zh. Eksp. Teor. Fiz.*, **79**, 1880 (1980).
15. Belyaeva N.N., Bredikhin V.I. *Kvantovaya Elekron.*, **11**, 633 (1984) [*Sov. J. Quantum Electron.*, **14**, 433 (1983)].
16. Miller A.M., Soustov L.V. *Kvantovaya Elektron.*, **16**, 61 (1989) [*Sov. J. Quantum Electron.*, **19**, 39 (1989)].
17. Swain J., Stokowski S., Milam D., Rainer F. *Appl. Phys. Lett.*, **40**, 350 (1982).
18. Cooper J.F., Singleton M.F. *Report LLNL*, UCRL-95904 (1987) (http://www.llnl.gov/tid/lof/documents/pdf/204713.pdf).
19. Woods B., Runker M., Yan M., Staggs M., Zaitseva N., Kozlowski M., De Yoreo J. *Report LLNL*, UCRL-JC-125368 (1996) (http://www.llnl.gov/tid/lof/documents/pdf/230901.pdf).
20. Salo V.I., Kolybayeva M.I., Puzikov V.M., Pritula I.M., Vasil'chuk V.G. *Proc. SPIE Int. Soc. Opt. Eng.*, **3359**, 549 (1998).
21. Atherton L.J., Rainer F., De Yoreo J.J., Thomas I.M., Zaitseva N., De Marco F. *Report LLNL*, UCRL-JC-115121 (1994) (http://www.llnl.gov/tid/lof/documents/pdf/224368.pdf).
22. Bespalov V.I., Bredikhin V.I., Ershov V.P., Katsman V.I., Kiseleva N.V., Kuznetsov S.P. *Kvantovaya Elektron.*, **9**, 2343 (1982) [*Sov. J. Quantum Electron.*, **12**, 1527 (1982)].
23. Andreev N.F., Bespalov V.I., Bredikhin V.I., Garanin S.G., Davydov V.S., Dolgopolov Yu.V., Katin E.V., Kuznetsov S.P., Kulikov S.M., Matveev A.Z., Rubakha V.I., Sukharev S.A. *Kvantovaya Elektron.*, **34**, 381 (2004) [*Quantum Electron.*, **34**, 381 (2004)].
24. Annenkov V.I., Bespalov V.I., Bredikhin V.I., Vinogradskii L.M., Gaidash V.A., Galakhov I.V., Garanin S.G., Ershov V.P., Zhidkov N.V., Zilberberg V.V., Zubkov A.V., Kalipanov S.V., et al. *Kvantovaya Elektron.*, **35**, 993 (2005) [*Quantum Electron.*, **35**, 993 (2005)].
25. Bespalov V.I., Bredikhin V.I., Ershov V.P., Katsman V.I., Lavrov L.A. *Izv. Akad. Nauk SSSR. Ser. Fiz.*, **51**, 1354 (1987).
26. Bespalov V.I., Bredikhin V.I., Ershov V.P., Katsman V.I., Lavrov L.A. *J. Cryst. Growth*, **82**, 776 (1987).
27. Andreev N.F., Bespalov V.I., Bredikhin V.I., Garanin S.G., Ginzburg V.N., Dvorkin K.L., Katin E.V., Korytin A.I., Lozhkarev V.V., Palashov O.V., Rukavishnikov N.N.,

Sergeev A.M., Sukharev S.A., Khazanov E.A., Yakovlev I.V. *Pis'ma Zh. Teor. Eksp. Fiz.*, **79**, 178 (2004).
28. Novikov M.A., Tertyshnik A.D. *Izv. Vyssh. Uchebn. Zaved. Ser. Radiofiz.*, **19**, 364 (1976).
29. Bondarenko N.G., Eremina I.V., Makarov A.I. *Kvantovaya Elektron.*, **5**, 841 (1978) [*Sov. J. Quantum Electron.*, **8**, 482 (1978)].
30. Craxton R.S. *IEEE J. Quantum Electron.*, **17**, 1771 (1981).
31. Auston D.H. *Ultrashort Light Pulses*. Ed. by S.L. Shapiro (Berlin – Heidelberg – New-York: Springer-Verlag, 1977) pp 121 – 201.
32. Lowdermilk W.H., Milam D. *IEEE J. Quantum Electron.*, **17**, 1888 (1981).
33. Koldunov M.F., Manenkov A.A., Pokotilo I.L. *Izv. Ross. Akad. Nauk. Ser. Fiz.*, **59**, 72 (1995).
34. Manenkov A.A. *Kvantovaya Elektron.*, **33**, 639 (2003) [*Quantum Electron.*, **33**, 639 (2003)].
35. Bredikhin V.I., Ershov V.P., Korolikhin V.V., Lizyakina V.N. *Kristallograf.*, **32**, 214 (1987).